




2022

The antihyperlipidemic equivalent combinatorial components from peel of *Citrus reticulata* 'Chachi'

Follow this and additional works at: <https://www.jfda-online.com/journal>

 Part of the [Food Science Commons](#), [Medicinal Chemistry and Pharmaceutics Commons](#), [Pharmacology Commons](#), and the [Toxicology Commons](#)



This work is licensed under a [Creative Commons Attribution-Noncommercial-No Derivative Works 4.0 License](#).

Recommended Citation

Xiao, Ping-Ting; Kuang, Yu-Jia; Liu, Shi-Yu; Xie, Zhi-Shen; Hao, Jin-Hua; and Liu, E-Hu (2022) "The antihyperlipidemic equivalent combinatorial components from peel of *Citrus reticulata* 'Chachi'," *Journal of Food and Drug Analysis*: Vol. 30 : Iss. 1 , Article 7.
Available at: <https://doi.org/10.38212/2224-6614.3388>

This Original Article is brought to you for free and open access by Journal of Food and Drug Analysis. It has been accepted for inclusion in Journal of Food and Drug Analysis by an authorized editor of Journal of Food and Drug Analysis.

The antihyperlipidemic equivalent combinatorial components from peel of *Citrus reticulata* ‘Chachi’

Ping-Ting Xiao ^{a,1}, Yu-Jia Kuang ^{a,1}, Shi-Yu Liu ^a, Zhi-Shen Xie ^b,
Jin-Hua Hao ^a, E-Hu Liu ^{a,*}

^a State Key Laboratory of Natural Medicines, China Pharmaceutical University, No. 24 Tongjia Lane, Nanjing, China

^b Academy of Chinese Medical Sciences, Henan University of Chinese Medicine, Zhengzhou, 450046, China

Abstract

Since the combinatorial components responsible for the antihyperlipidemic activity of *Citrus reticulata* ‘Chachi’ (CRC) peels remains unclear, we herein developed a bioactive equivalence oriented feedback screening method to discover the bioactive equivalent combinatorial components (BECCs) from CRC peels. Using palmitic acid (PA)-stimulated hepatocyte model, a combination of 5 polymethoxyflavones (PMFs) including tangeretin, sinensetin, nobiletin, 5,7,8,4'-tetramethoxyflavone and 3,5,6,7,8,3',4'-heptamethoxyflavone was identified to be responsible for the antihyperlipidemic effect of CRC peels. *Via* evaluation of combination effect by combination index (CI), these 5 PMFs were found to take effect *via* a synergistic mode. Our data indicated that the antihyperlipidemic mechanism of PMF combination was associated with the inhibition of fatty acid and cholesterol synthesis, and inflammation. Also, the PMF combination exhibited robust antihyperlipidemic effects in HFD-fed rats *in vivo*. Our study offers evidence-based data to uncover the pharmacological effect of CRC peels.

Keywords: Antihyperlipidemic, BECCs, *Citrus reticulata* ‘Chachi’, Polymethoxyflavones

1. Introduction

Citrus reticulata ‘Chachi’ (CRC), one of the varieties of *Citrus reticulata* Blanco, is mainly planted in Xinhui County, Guangdong Province, China [1]. The dried peels of CRC have been commonly consumed in snack, functional foods, popular tea, traditional spice and flavoring for centuries [2]. Phytochemical studies demonstrated that the major components of CRC peels are dietary flavonoids, which are generally categorized into two groups: flavanone glycosides (primarily hesperidin) and polymethoxyflavones (PMFs, primarily nobiletin and tangeretin) [1,3–5]. Pharmacological studies indicated that the CRC extracts exhibited profound effects in prevention of hyperlipidemia, obesity and type 2 diabetes [6,7]. However, due to the complex ingredients in CRC peels, the combinatorial components responsible for the antihyperlipidemic activity of CRC peels have not been systematically confirmed.

Bioactive equivalent combinatorial components (BECCs) are the combinatorial components accounting for the whole efficacy of herbal medicines [8], and the identification of BECCs acting in a synergistic and/or additive mode is a key step to finally uncovering the multiple-target mechanism of herbal medicines [9,10]. The bioactive equivalence oriented feedback screening method provides a promising strategy for discovering BECCs from complex medicines or foods.

The current study aims to identify the antihyperlipidemic equivalent combinatorial components from CRC peels *via* a bioactive equivalence oriented feedback screening approach. The antihyperlipidemic activities of BECCs identified were evaluated in both in PA-stimulated HL7702 cells *in vitro* and in HFD-fed rats *in vivo*. The interactive mode of compounds in combination and the antihyperlipidemic mechanism of BECCs were also investigated. The uncovering the BECCs from CRC

Received 9 July 2021; Received 1 September 2021; Accepted 13 October 2021.
Available online 15 March 2022.

* Corresponding author at: Fax: +86 25 83271379.
E-mail address: liuehu2011@163.com (E.-H. Liu).

¹ These Authors contributed to this paper equally.

<https://doi.org/10.38212/2224-6614.3388>

2224-6614/© 2021 Taiwan Food and Drug Administration. This is an open access article under the CC-BY-NC-ND license (<http://creativecommons.org/licenses/by-nc-nd/4.0/>).

peels will provides insights to the clinical application of citrus products.

2. Materials and methods

2.1. Reagents and materials

A Milli-Q water purification system (Millipore, Bedford, MA, USA); Agilent 1260 Series HPLC (Agilent Technologies, USA); Thermo BDS HYPERSIL C18 column (250 × 4.6 mm, 5 μm, Thermo, USA); Agilent 1100 Series HPLC (Agilent Technologies, USA); YMC-Pack ODS-A semi-preparative column (250 × 10 mm, 5 μm); Nile red (Macklin, Shanghai, China); lovastatin (LOV; Aladdin, China); BODIPY 493/503 (4,4-difluoro-1,3,5,7,8-pentamethyl-4-bora-3a, 4-diaza-s-indacene, Molecular Probes, Invitrogen); 5,7,8,4'-Tetramethoxyflavone (TET) (≥98%, Push bio-technology, China); narirutin (NAR), didymin (DID), nobiletin (NOB), sinensetin (SIN), 3,5,6,7,8,3',4'-heptamethoxyflavone (HMF) and synephrine (SYN) (≥98%, Biopurify Phytochemicals, China); naringin (NAN) and hesperidin (HES) (≥98%, Must bio-technology, China); neohesperidin (NEO), 5-hydroxy-6,7,8,3',4'-Pentamethoxyflavone and tangerine (TAN) (≥98%, prepared in our laboratory); TRIzol, high capacity cDNA reverse transcription kit and SYBR-green (Vazyme, Nanjing, China); quantitative PCR (Roche, Basel, Switzerland); HL7702 (ATCC, USA); Dulbecco's modified Eagle's medium (DMEM; Corning, USA). Fetal bovine serum (FBS; Gibco, USA); dimethyl sulfoxide (DMSO; Sigma, Louis, MO, USA.).

2.2. Plant materials

CRC peel samples were collected from Xinhui County (Guangdong province, China) in December.

2.3. Sample preparation and HPLC analysis

2 g CRC peels were cut into slices and immersed in 14 folds 70% ethanol for 90 min. The peels were then extracted twice under reflux, each for 2 h. After filtered, the extract was freeze-dried [11]. For quantification of the 6 bioactive flavonoids in CRC peels, an amount of 2.5 mg freeze-dried powder was accurately weighed, dissolved in 1 mL methanol and further analyzed using the Agilent 1260 Series HPLC. Chromatographic separation was conducted on an Thermo BDS HYPERSIL C18 column (250 × 4.6 mm, 5 μm). The mobile phase consisted of water with 0.1% formic acid (A) and acetonitrile (B) using a gradient elution mode of 25%–50% B at 0–3 min, 50%–58% B at 3–7 min,

58% B at 7–11 min, 58%–90% B at 11–15 min, with 8 min post time. 6 flavonoids were monitored at 330 nm, with a sample injection volume of 10 μL. The quantification was also carried out by integration of the peak using an external standard method.

2.4. Trapping and preparing candidate BECCs

To obtain the combination of candidate BECCs, we applied Agilent 1100 series HPLC system to collect fractions. The HPLC separation was performed on a YMC-Pack ODS-A semi-preparative column (250 × 10 mm, 5 μm) with a flow rate of 2 mL/min, the BECCs and the remaining part were collected at two different positions. The samples were reconstituted at a concentration as in original CRC peels for method validation and bioactivity assay. The Agilent 1260 Series HPLC [11]. Chromatographic separation was conducted on an Thermo BDS HYPERSIL C18 column (250 × 4.6 mm, 5 μm). The mobile phase consisted of water with 0.1% formic acid (A) and acetonitrile (B) using a gradient elution mode of 25%–50% B at 0–3 min, 50%–58% B at 3–7 min, 58% B at 7–11 min, 58%–90% B at 11–15 min, with 8 min post time.

2.5. Bioactive equivalence oriented feedback screening method

Firstly, the candidate BECCs in CRC peels are quantitated according to a predefined selection criterion. Then, the candidate BECCs are trapped and prepared, the remaining part is obtained simultaneously. Lastly, the antihyperlipidemic activity of candidate BECCs and CRC peels were evaluated and compared [12]. Bioactive equivalence was evaluated by calculating 90% confidence interval of the ratio between the efficacies of candidate BECCs and CRC peels (two one-sided *t* test). If the 90% confidence interval of relative efficacy compared to original CRC peels fell within the range of 70%–143%, the candidate BECCs were considered to be a bioactive equivalent with CRC peels [13].

2.6. Cell lines

HL7702 were grown in DMEM supplemented with 100 U/mL penicillin, 100 μg/mL streptomycin, and 10% (v/v) FBS at 37 °C in a 5% CO₂ incubator.

2.7. Cell viability assay

HL7702 cells were seeded in a 96-well plate at a density of 2.5×10^4 cells/well. After 18 h, the cells

were administrated with signal compound at the concentration of 5, 10, 20, 40 and 80 μM , or CRC peel extract (0–600 $\mu\text{g}/\text{mL}$), mixture of reference compounds (MRCs), BECCs respectively for 24 h. 3-(4,5-dimethylthiazol-2-yl)-2,5-diphenyltetrazolium-bromide (MTT) was added for 4 h, and detected the absorbance at 490 nm by Synergy 2 MultiFunction Microplate Reader (Bio-Tek Instruments, Winooski, VT, USA).

2.8. Palmitic acid (PA)-induced steatosis

HL7702 cells were seeded in 6-well plates at 2×10^5 cells per well for 18 h, then incubated with 100 μM PA in normal culture medium as the model group together with test compounds or not for 24 h.

2.9. Nile-red staining

Cells were fixed with 4% paraformaldehyde (PFA) for 30 min, stained with 0.5 $\mu\text{g}/\text{mL}$ Nile-red after wash for 30 min at room temperature. Images were captured with fluorescence microscopy.

2.10. BODIPY (493/503) staining

Cells were fixed with 4% PFA for 30 min, stained with BODIPY (493/503) after wash at a concentration of 1 $\mu\text{g}/\text{mL}$ at 37 °C for 15 min. Images were captured with fluorescence microscopy.

2.11. Fluorescence quantification

For quantification of intracellular lipid abundance, red or green pseudocolors that showed the BODIPY (493/503) or Nile-Red signal were measured by Image-Pro Plus 6.0 (Media Cybernetics, USA) and calculated. The intensity of control cell was arbitrarily defined as 1, against which the intensities of different treated cells were normalized.

2.12. Evaluation of combination effect by combination index (CI)

CI was applied to investigate the multi-component interactions among the active compounds. The investigation of interaction in combinations involves establishing dose-effect curves for single compounds alone and multiple combinations of agents. To calculate the CI values, the ability for inhibiting the lipid level in PA-induced HL7702 cells of NOB, SIN, TAN, TNT, HMF and combinations of 5 PMFs were tested at various concentrations. Based on the content of single PMF in combination, the effect

values of the above groups were then introduced into CompuSyn software (ComboSyn Inc., USA) and the CI values could be calculated. Generally, CI values <0.9 are considered synergistic, >1.1 are antagonistic, and values 0.9 to 1.1 are nearly additive [14].

2.13. The extraction and quantification of PMFs in CRC peels

CRC peels were cut into slices and immersed in 14 folds 70% ethanol for 90 min, and extracted twice under reflux, each for 2 h, then PMFs were enriched by HPD-450, and then freeze-dried. For quantification of 5 PMFs in PMF combination, an amount of 1 mg freeze-dried powder was accurately weighed, dissolved in 1 mL methanol and further analyzed using the Agilent 1260 Series HPLC [11]. Chromatographic separation was conducted on an Thermo BDS HYPERSIL C18 column (250 \times 4.6 mm, 5 μm). The quantification was also carried out by integration of the peak using an external standard method.

2.14. Real-time quantitative PCR

Total RNA was extracted and isolated using TRIzol and reversed transcribed by high capacity cDNA reverse transcription kit according to the manufacturer's instructions. Gene expression was measured by quantitative PCR using SYBR-green. The mRNA expression of respective genes was normalized to the level of 18S rRNA mRNA and quantified by the $2^{-\Delta\Delta\text{Ct}}$ method. Primers sequences were shown in Table S1.

2.15. Immunoblotting

Cells were lysed in RIPA buffer supplemented with a protease inhibitor cocktail. Protein extracts were separated on 8%–10% SDS-PAGE gels and transferred onto nitrocellulose membranes. Membranes were blocked by incubation for 1 h with 5% non-fat milk, and blotted overnight with the specific antibodies at 4 °C followed by the corresponding secondary antibodies. Then, signals were detected with Tanon-5200 Chemiluminescent Imaging System (Tanon, Shanghai, China). Band densitometry was performed using by ImageJ 1.46r software (National Institute of Health, USA), and relative protein expression was determined by normalizing to β -actin. The following antibodies were used: SREBP-2 (#ab30682, Abcam, USA); SREBP-1 (#sc-8984) and β -actin (#sc-81178) (Santa Cruz

Biotechnology, USA); TNF- α (#A0277) (Abclonal, China); anti-rabbit or mouse secondary antibodies (ZSGB-BIO, Beijing, China).

2.16. Animals

We obtained 6-week-old Sprague–Dawley rats from Sino-British SIPPR/BK Lab Animal Ltd (Shanghai, China), and kept them under a 12-h light/dark cycle. The rats were divided into three groups and fed either a normal chow diet or high-fat diet (normal chow supplemented with 13% pork oil, 7% soybean oil, 5% yolk powder, 8% sugar, 1% cholesterol, 0.5% gall salt) for 10 weeks. Rats in PMFs treated groups, were fed a HFD for 4 weeks, then once daily oral gavaged with 40 mg/kg PMFs for another 6 weeks with continuing a HFD feeding. The PMFs were dissolved in 0.5% CMC-Na.

The procedures for experiments and animal care were approved by the Institutional Animal Care and Use Committee of China Pharmaceutical University (Nanjing, China). Animal testing and research conforms to all relevant ethical regulations. All institutional and national guidelines for the care and use of laboratory animals were followed.

2.17. Biochemical measurements

Serum total cholesterol (TC), triglyceride (TG), low-density lipoprotein cholesterol (LDL-c) and high-density lipoprotein cholesterol (HDL-c) levels were measured by Automatic Biochemistry Analyzer (Roche Cobas 8000 modular analyzer Series, Roche Diagnostics GmbH, Mannheim, Germany) according to the manufacturer's instructions.

2.18. Histological analysis of liver and adipose

Livers, epididymal adipose tissues (WAT) and interscapular brown adipose tissues (BAT) were fixed in 4% PFA and embedded in paraffin wax. Paraffin sections (5 μ m) were stained with haematoxylin and eosin (H&E). Sections were examined under digital pathological section scanner (Nano-Zoomer 2.0 RS, Hamamatsu, Japan).

2.19. Statistical analysis

Statistical analysis was performed with GraphPad Prism 7.0 software. The results are expressed as the mean \pm standard error of the mean (SEM). Data were compared by one-way ANOVA followed by a Dunnett

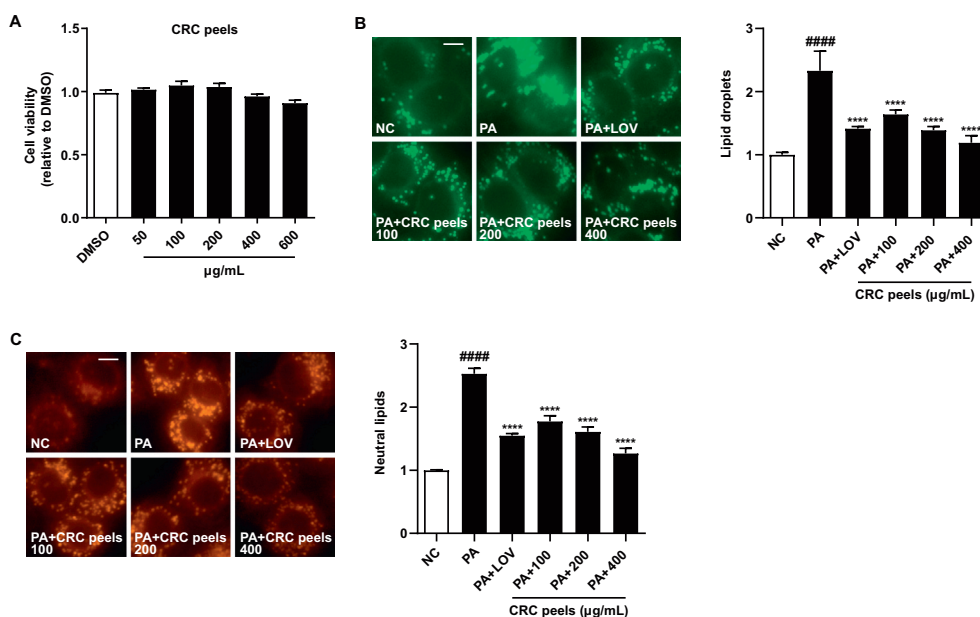


Fig. 1. Antihyperlipidemic effects of CRC peels in PA-stimulated HL7702 lipid deposition. (A) HL-7702 cells were treated with indicated concentrations of CRC peels for 24 h. Cell viability was measured by MTT assay, $n = 5$. (B) Measurement (left panel) and the quantification (right panel) of lipid content by BODIPY (493/503) Staining in HL7702 cells 24 h after treatment with DMSO, PA alone, and PA together with LOV or CRC peels, $n = 6$. (C) Measurement (left panel) and the quantification (right panel) of lipid content by Nile Red fluorescence in HL7702 cells 24 h after treatment either with DMSO, PA alone, and PA together with LOV or CRC peels, $n = 6$. Error bars represent mean \pm SEM. Comparisons between two groups were analyzed by using a two-tailed Student's t test, and those among three or more groups by using one-way analysis of variance (ANOVA) followed by Dunnett's post hoc tests. ****: $p < 0.0001$ vs. the PA group, #####: $p < 0.0001$ vs. the NC group. (NC, normal control; PA, palmitic acid; LOV, lovastatin).

post-hoc test. The differences were considered statistically significant when $p < 0.05$.

For bioactive equivalence assessment, all the bioassay results were transformed to efficacy value. Bioactive equivalence was evaluated by calculating 90% confidence interval of the ratio between the efficacies of candidate BECCs and CRC peels. If the 90% confidence interval of relative efficacy compared to original CRC peels fell within the range of 70–143% [12], the candidate BECCs were considered to be a bioactive equivalent with original CRC peels.

3. Results and discussion

3.1. CRC peels alleviates PA-stimulated lipid accumulation in hepatocytes

Chemical studies show that the CRC peels contain abundant PMFs. The contents of nobiletin,

tangeretin and 5-hydroxy-6,7,8,3',4'-pentamethoxyflavone were much higher in CRC peels than in other citrus cultivars [15]. PA, a saturated fatty acid, can cause lipid accumulation and the release of inflammatory extracellular vesicles in hepatocytes. To investigate the antihyperlipidemic effects of CRC peels, we stimulated the lipid deposition with PA in HL7702 hepatocytes, then cells were treated with various concentrations of extract of CRC peels. Our data indicated that no obvious cytotoxicity was observed until the concentration of CRC peels up to 600 $\mu\text{g}/\text{mL}$ in HL-7702 cells (Fig. 1A). Both BODIPY (493/503) Staining and Nile Red fluorescence assays indicated that CRC peels significantly inhibited the PA-induced lipid accumulation in a dose-dependent manner (Fig. 1B–C). These data suggested that CRC peels treatment could reduce lipid contents in hepatocytes. The concentration of 400 $\mu\text{g}/\text{mL}$ (peel

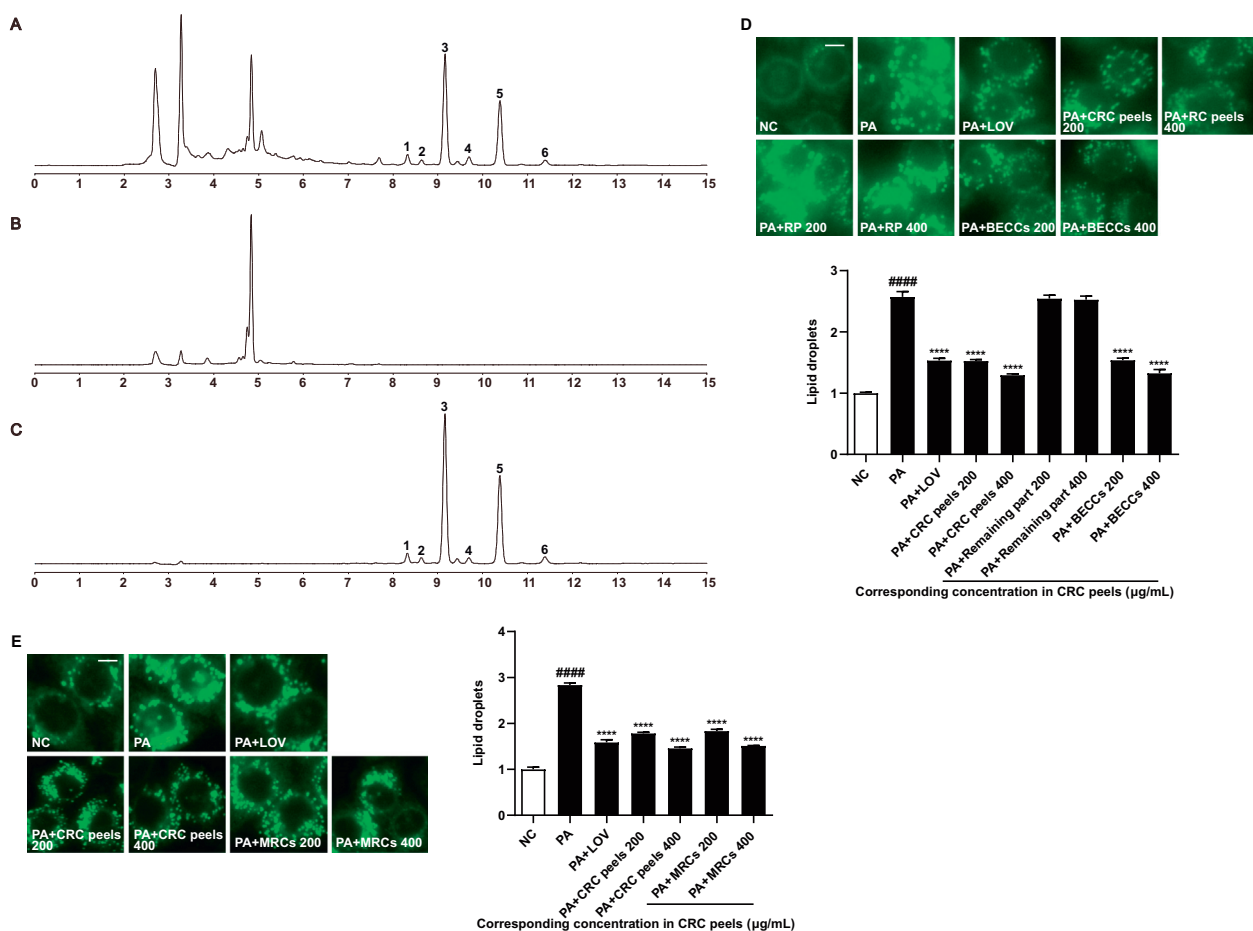


Fig. 2. *In vitro* activity assays of candidate BECCs. (A–C) Validation of candidate BECCs by HPLC. (A) Chromatogram of CRC peels. (B–C) Chromatogram of remaining part (B) and candidate BECCs (C). (1) SIN, (2) TET, (3) NOB, (4) HMF, (5) TAN, (6) 5-hydroxy-6,7,8,3',4'-pentamethoxyflavone. (D) Measurement (top panel) and the quantification (bottom panel) of lipid content by BODIPY (493/503) Staining in HL7702 cells 24 h after treatment with DMSO, PA alone, and PA together with LOV, CRC peels, remaining part or BECCs, respectively, $n = 6$. (E) Measurement (left panel) and the quantification (right panel) of lipid content by BODIPY (493/503) Staining in HL7702 cells 24 h after treatment with DMSO, PA alone, and PA together with LOV, CRC peels or MRCs, respectively, $n = 6$. Error bars represent mean \pm SEM. Comparisons between two groups were analyzed by using a two-tailed Student's *t* test, and those among three or more groups by using one-way analysis of variance (ANOVA) followed by Dunnett's post hoc tests. ****: $p < 0.0001$ vs. the PA group, ####: $p < 0.0001$ vs. the NC group; NC, normal control; PA, palmitic acid; LOV, lovastatin; BECCs, bioactive equivalent combinatorial components; MRCs, mixture of reference compounds; 3,5,6,7,8,3',4'-heptamethoxyflavone; TAN, tangerine; SIN, sinensetin; NOB, nobiletin; TET, 5,7,8,4'-tetramethoxyflavone; MRCs, mixture of reference compounds).

Table 1. The content of 6 PMFs in CRC peels.

Compounds	The concentrations of compounds in 400 $\mu\text{g/mL}$ CRC peels ($\mu\text{g/mL}$)
sinensetin	0.13
5,7,8,4'-tetramethoxyflavone	0.08
nobiletin	3.09
3,5,6,7,8,3',4'-heptamethoxyflavone	1.25
tangerine	1.31
5-hydroxy-6,7,8,3',4'-pentamethoxyflavone	0.18

extract) was applied for further identification of BECCs in CRC peels.

3.2. In vitro assessment of bioactive equivalence between candidate BECCs and CRC peel extract

Given that CRC peels contain complex and relatively unrefined compounds [4,16], it is necessary to investigate the antihyperlipidemic equivalent

combinatorial components from CRC peels. Thus, the described bioactive equivalence oriented feedback screening method was applied to discover BECCs from CRC peels. Both candidate BECCs and the remaining parts of extract were prepared and used for bioactivity evaluation. Since the PMFs such as NOB, are reported to have antihyperlipidemic activity [17], we hypothesize PMFs are the candidate BECCs in CRC peels. To verify the hypothesis, the candidate BECCs (the combination of 6 PMFs) and the remaining part were firstly trapped, prepared and further confirmed from CRC peels completely by employing HPLC (Fig. 2A-C). Their antihyperlipidemic activities were then evaluated using PA-stimulated hepatocytes. Both the candidate BECCs and the remaining part showed no discernible toxicity in HL-7702 cells (Fig. S1A-B). The candidate BECCs showed a similar effect of decreasing the lipid content as CRC peels (Fig. 2D), whereas the remaining part did not influence the lipid content. For the bioactive equivalence assessment, 90% confidence interval showed that the

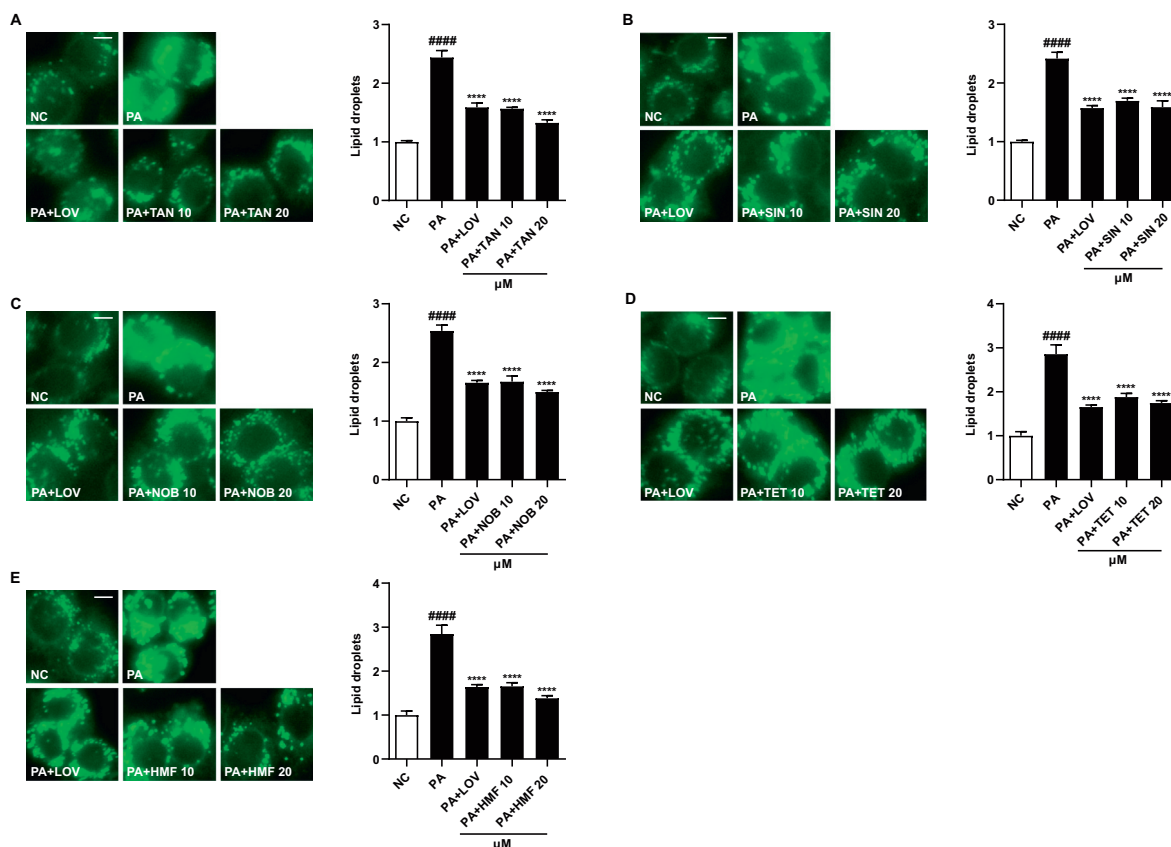


Fig. 3. Chemical family classification-based screening of antihyperlipidemic compounds from CRC peels. (A–E) Measurement (left panel) and the quantification (right panel) of lipid content by BODIPY (493/503) Staining in HL7702 cells 24 h after treatment with DMSO, PA alone, and PA together with LOV or (A) TAN, (B) SIN, (C) NOB, (D) TET, (E) HMF, $n = 6$. Error bars represent mean \pm SEM. Comparisons between two groups were analyzed by using a two-tailed Student's t test, and those among three or more groups by using one-way analysis of variance (ANOVA) followed by Dunnett's post hoc tests. ****: $p < 0.0001$ vs. the PA group, #####: $p < 0.0001$ vs. the NC group. (NC, normal control; PA, palmitic acid; LOV, lovastatin; HMF, 3,5,6,7,8,3',4'-heptamethoxyflavone; TAN, tangerine; SIN, sinensetin; NOB, nobiletin; TET, 5,7,8,4'-tetramethoxyflavone).

ratios of efficacies between CRC peels and BECCs were within the acceptance range of 70–143% (Table S2). Thus, the candidate BECCs could be considered as BECCs of CRC peels.

To exclude the interference of any undetected microconstituents in the collected BECCs, we prepared a mixture of reference compounds (MRCs) by mixing the 6 PMFs reference compounds (compound 1–6 in Fig. 2A–C, Table 1) according to the content of these compounds in CRC peels for bioactivity validation. The results indicated that the MRCs and CRC peels showed the similar protective effects with no discernible toxicity (Fig. 2E and Fig. S1C). These results indicate that PMFs are the primary antihyperlipidemic constituents in CPC peels, and the antihyperlipidemic effect of candidate BECCs is comparable to that of CRC peels *in vitro*.

The bioactive equivalence assessment data were also consistent with that of candidate BECCs; 90% confidence interval of efficacies between CRC peels and MRCs lay within 70–143% (Table S2). Together, these results demonstrated that the antihyperlipidemic effect of the MRCs was comparable to that of CRC peels, and the PMFs combination could be considered as BECCc of CRC peels.

3.3. Chemical family classification-based screening

To validate the antihyperlipidemic effect of PMFs, 6 PMFs including SIN, TET, NOB, TAN, HMF and 5-hydroxy-6,7,8,3',4'-Pentamethoxyflavone, together with 5 flavanone glycosides (NAN, NAR, HES, NEO and DID), and 1 alkaloid SYN were selected for antihyperlipidemic evaluation using PA-stimulated

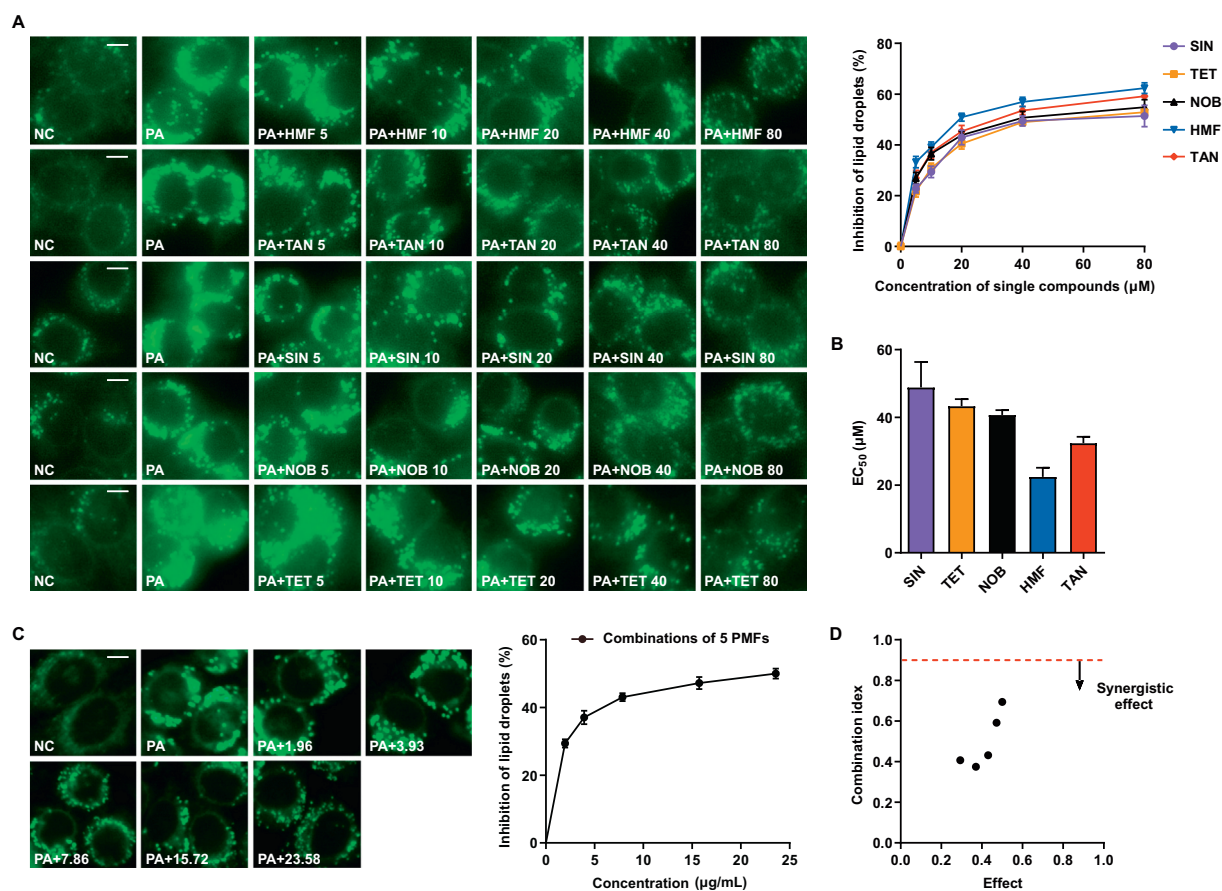


Fig. 4. Combination index and dose-dependent inhibition of PA-induced lipid deposition by single active compounds or compound combinations. (A) Measurement (left panel) and the dose-effect curves (right panel) of NOB, SIN, TAN, HMF, TET in inhibition of lipid content by BODIPY (493/503) Staining in HL7702 cells 24 h after treatment with PA alone, and PA together with NOB, SIN, TAN, HMF or TET, respectively, $n = 6$. (B) EC₅₀ of 5 PMFs, $n = 3$. (C) Measurement (left panel) and the dose-effect curves (right panel) in inhibition of combinations of 5 PMFs of lipid content by BODIPY (493/503) Staining in HL7702 cells 24 h after treatment with PA alone, and PA together with combinations of 5 PMFs, $n = 6$. (D) Combination index. The combination index was calculated using CompuSyn software. $0 < CI < 0.9$ indicated a synergism effect. Error bars represent mean \pm SEM. (NC, normal control; PA, palmitic acid; HMF, 3,5,6,7,8,3',4'-heptamethoxyflavone; TAN, tangerine; SIN, sinensetin; NOB, nobiletin; TET, 5,7,8,4'-tetramethoxyflavone).

HL7702 cells. The results indicated that all the tested compounds showed no discernible toxicity in HL7702 cells except 5-hydroxy-6,7,8,3',4'-Pentamethoxyflavone (Fig. S2 and Fig. S3). As shown in Fig. 3 and Fig. S4, all the 5 PMFs significantly reduced lipid droplets in HL7702 hepatocytes in a concentration-dependent manner, as measured by BODIPY (493/503) Staining and lipid content by Nile Red fluorescence. The 5 flavanone glycosides including NAN, NAR, HES, NEO and DID, and the alkaloid SYN did not affect the lipid content (Fig. S5 and Fig. S6). These results demonstrated that PMFs were primary responsible for the antihyperlipidemic effects of CRC peels.

3.4. Characterization of interactive mode among PMFs

Next, using the PA-stimulated HL7702 cells, we investigated the dose–effect relationship of single PMF and evaluated the interactive mode among PMFs. The mixed standards of combinations of 5 PMFs (NOB, SIN, TAN, TNT and HMF) were prepared, of which the concentrations were the same as those in CRC peels. To calculate the CI values, the lipid inhibition in PA-stimulated HL7702 cells of NOB, SIN, TAN, TNT, HMF and combinations of 5 PMFs were tested at various concentrations. Both BODIPY (493/503) Staining and Nile Red fluorescence assays indicated that all the PMFs and combinations of 5 PMFs decreased the lipid content in a concentration-dependent manner (Fig. 4A–C, Fig. S7A–C) and the compound HMF, which had an EC_{50} of $\sim 22.45 \mu\text{M}$, showed the most potent lipid-lowering activity (Fig. 4B, Fig. S7B). Then, a CI method was used for assessing the nature of interaction (synergistic, additive, or antagonistic effect). The effect values of the above groups were introduced into CompuSyn software to obtain the CI values. As showed in Fig. 4D, Fig. S7D and Table 2, most of the CI values located in the range of 0–0.9, indicating a synergism effect among NOB, SIN, TAN, TNT and HMF. Long et al., evaluated the interactive mode of 6 compounds in combination responsible for anti-inflammatory activity of Cardiotonic Pill and found that these 6 compounds

take effect *via* an additive mode [8]. Of interest, our results showed that the PMFs in combination exert effect in a synergistic mode.

3.5. BECCs exerts antihyperlipidemic effects via inhibition of inflammation, fatty acid and cholesterol synthesis

We next preliminarily investigate the antihyperlipidemic mechanism of BECCs. Sterol regulatory element-binding proteins (SREBPs) play important roles in regulating lipid homeostasis and are considered as targets for the treatment of metabolic diseases [18]. Our data indicated that BECCs treatment significantly reduced expressions of SREBP target genes, such as cholesterol metabolism genes *DHCR24*, *PSCK9*, *HMGCR*, and *SREBP-2*, as well as fatty acid metabolism genes *SREBP-1c*, *FASN*, *ACCI*, *ACLY*, and *SCD1* (Fig. 5A–B). However, BECCs did not affect the mRNA expression of *ABCA1*, *ABCG5* and *CYP7A1*, which mediated the efflux and clearance of cholesterol and fatty acid [19–21], as well as *PPAR α* , *CPT1* and *LPL*, which mediated the fatty acid oxidation [22,23] (Fig. 5C–D). Moreover, BECCs significantly reduced the mRNA expression of tumor necrosis factor- α (*TNF- α*) and interleukin-1 β (*IL-1 β*) (Fig. 5E). BECCs treatment also decreased the protein expression of n-SREBP-1, n-SREBP-2 and *TNF- α* , but did not activate pre-SREBP-1 and pre-SREBP-2 (Fig. 5F). We also found that different single PMF may not affect the same molecular mechanism, for example, HMF down-regulated the expression of *SREBP-2*, *HMGCS1*, *DHCR24*, *MVK*, *SREBP-1C*, *FASN*, *ACC2*, *FADPS-2* and *TNF- α* , while SIN decreased *SREBP-1C*, *HMGCS1*, *DHCR24*, *MVK* and *TNF- α* mRNA levels (Fig. S8). Together, these results indicate that BECCs ameliorate hyperlipidemia by inhibiting the synthesis of cholesterol and fatty acids, as well as inflammatory.

3.6. BECCs exhibits robust antihyperlipidemic effects in HFD-fed rats

The antihyperlipidemic activity of BECCs was further verified *in vivo*. We firstly prepared the PMFs

Table 2. The interactions among 5 PMFs.

	Lipid droplets			Neutral lipids		
	EC_{50} ($\mu\text{g}/\text{mL}$)	95% confidence interval	CI	EC_{50} ($\mu\text{g}/\text{mL}$)	95% confidence interval	CI
Combinations of 5 PMFs	12.69	9.80–16.50	0.62	12.54	9.74–16.23	0.59

combination by microporous resin chromatography, and the 5 major PMFs (SIN, TET, NOB, TAN and HMF) made up the major components of purified extracts with the purity 74.61% (*w/w*) (Fig. 6A-B and Table S3). HFD-fed rats were used as the model to address whether PMFs displays a protective effect against hyperlipidemia *in vivo*. As shown in Fig. 6C, PMFs treatment lowered lipid accumulation in liver, reduced the cell size of white adipocyte tissue and interscapular brown adipose tissues. Moreover, the serum TC, TG, and LDL-c were dramatically reduced, whereas the significant increase in HDL-c

was not observed in PMFs-treated rats (Fig. 6D-G). These results indicate that PMFs combination exhibits robust efficacy against hyperlipidemia in HFD-fed rats. Recently, HMF was reported to prevent obesity in high-fat diet-induced rats by regulation of the expression of lipid metabolism-related and inflammatory response related genes [24]. Indeed, a purified PMF-rich extract from CRC was shown to be protective against high-fat feeding in a microbiota-dependent manner, suggesting that the extract may be a therapeutic prebiotic agent for the treatment of metabolic disease [25].

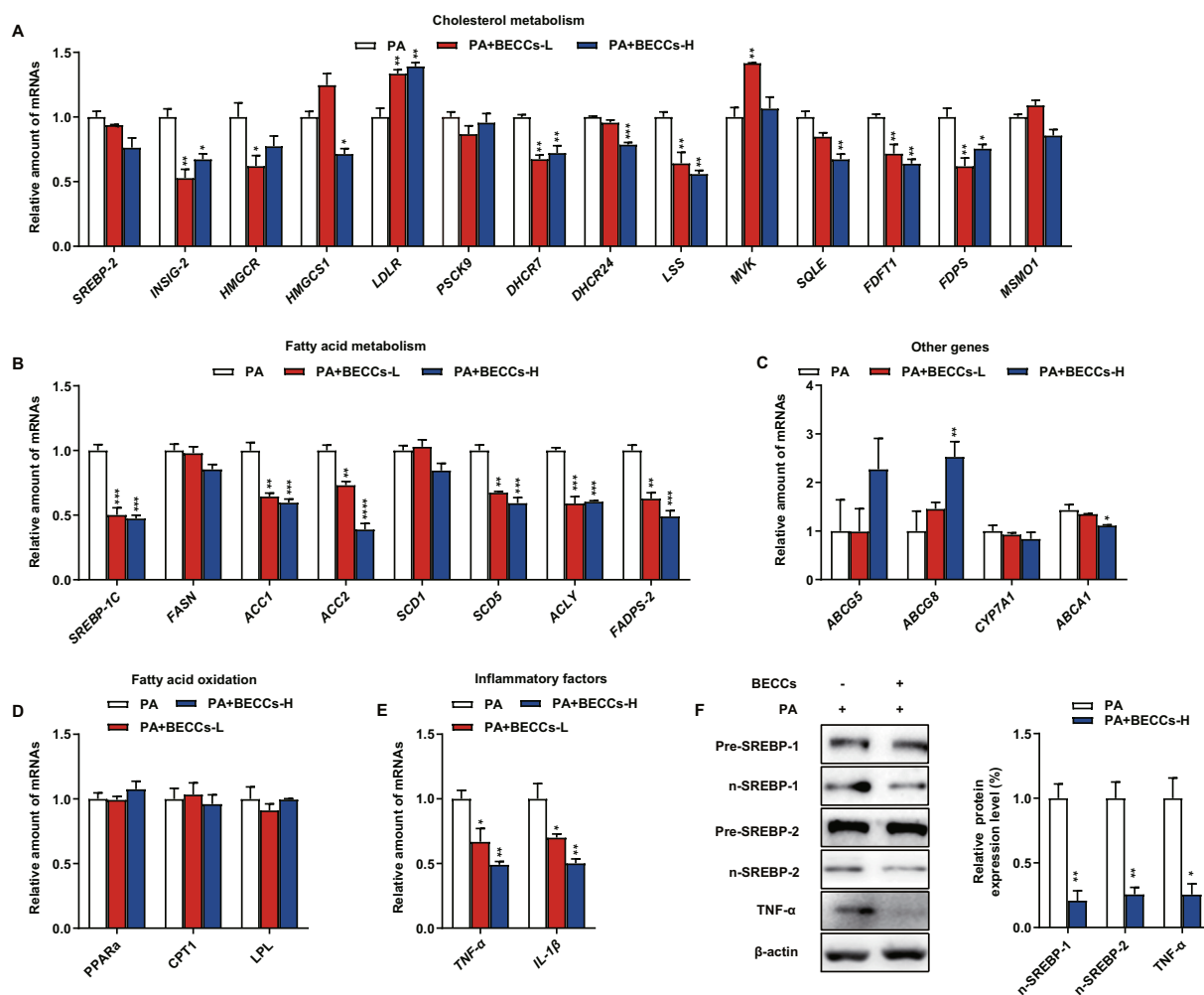


Fig. 5. Effects of BECCs on the expression of genes involved in lipid homeostasis. (A–E) Effect of BECCs on (A) cholesterol metabolism, (B) fatty acid metabolism, (C) other genes, (D) fatty acid oxidation, (E) inflammatory factors. HL-7702 cells were treated with DMSO, PA alone, and PA together with indicated concentrations of BECCs (7.86 $\mu\text{g}/\text{mL}$, 15.72 $\mu\text{g}/\text{mL}$) for 24 h. (F) Western blot (left panel) and quantification (right panel) of TNF- α and nuclear SREBP protein expression in HL7702 cells, β -actin levels served as loading control, $n = 3$. HL-7702 cells were treated with DMSO, PA alone, and PA together with BECCs (15.72 $\mu\text{g}/\text{mL}$) for 24 h. Error bars represent mean \pm SEM. Comparisons between two groups were analyzed by using a two-tailed Student's *t* test, and those among three or more groups by using one-way analysis of variance (ANOVA) followed by Dunnett's post hoc tests. *: $p < 0.05$, **: $p < 0.01$, ***: $p < 0.001$, ****: $p < 0.0001$ vs. the PA group. (PA, palmitic acid; BECCs, bioactive equivalent combinatorial components).

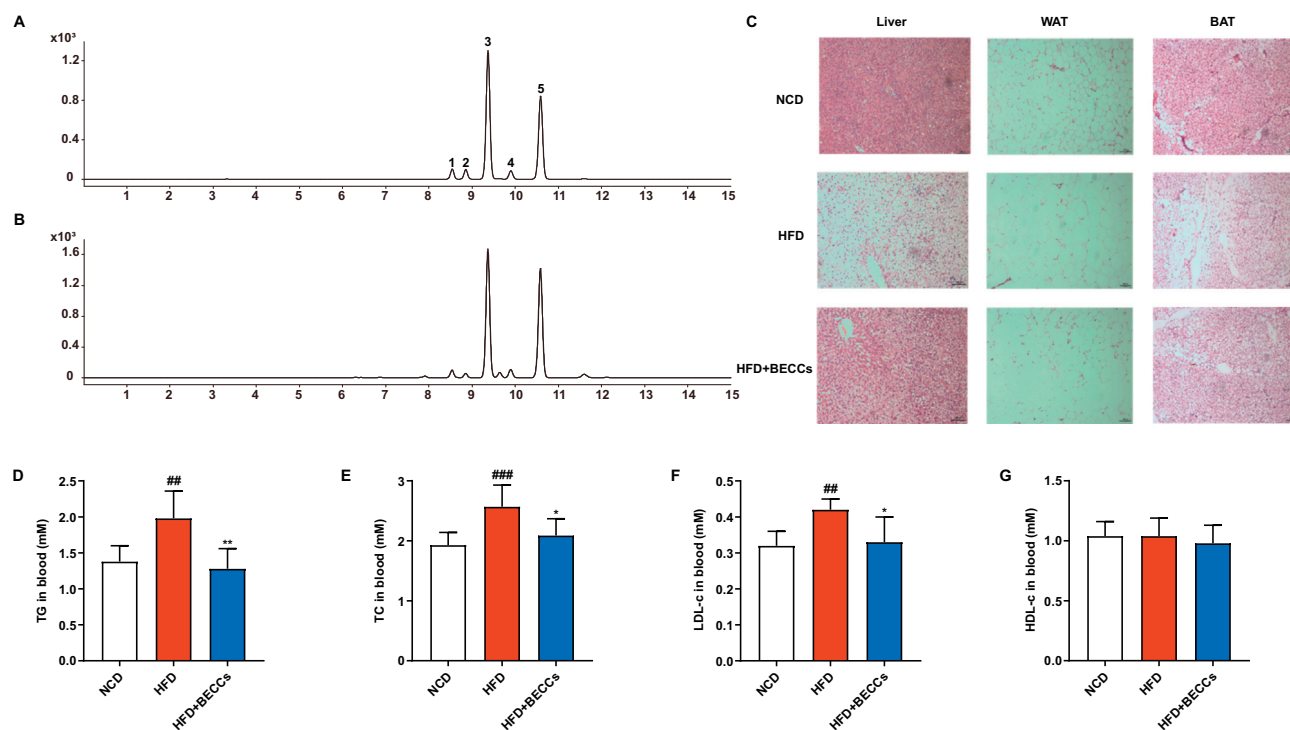


Fig. 6. PMFs exhibits robust metabolic protective effects in HFD-fed rats. (A) HPLC chromatogram of 5 PMFs. Detection was at 330 nm. Peak: (1) SIN, (2) TET, (3) NOB, (4) HMF, (5) TAN. (B) HPLC chromatogram of 5 flavonoids in PMF combination. Vehicle, or PMFs (40 mg/kg/day) was administered to HFD rats by gastric irrigation once daily for 6 weeks. The mice were finally sacrificed and subjected to various analyses as indicated below. (C) Representative pictures of H&E-stained liver, white adipose tissue (WAT) and interscapular brown adipose tissues (BAT) (scale bar, 100 μ m). (D–G) Total TC, TG, LDL-c, and HDL-c levels in blood, $n = 10$. Error bars represent mean \pm SEM. *: $p < 0.05$, **: $p < 0.01$ vs. the HFD group, ##: $p < 0.01$, ###: $p < 0.001$ vs. the NCD group (assessed by Student's t test). (HMF, 3,5,6,7,8,3',4'-heptamethoxyflavone; TAN, tangerine; SIN, sinensetin; NOB, nobiletin; TET, 5,7,8,4'-tetramethoxyflavone; TG, triglyceride; TC, total cholesterol; LDL-c, low-density lipoprotein cholesterol; HDL-c, high-density lipoprotein cholesterol).

4. Conclusion

In the present study, based on the bioactive equivalence oriented feedback screening method, a combination of 5 PMFs (SIN, TET, NOB, TAN and HMF) was identified as the antihyperlipidemic equivalent combinatorial components from CRC peels. The PMFs combination exhibits robust antihyperlipidemic activities both in PA-stimulated HL7702 cells *in vitro* and in HFD-fed rats *in vivo*. Moreover, the combination exerts antihyperlipidemic effect *via* a synergistic mode, and the mechanism is attributed to the inhibition of fatty acid and cholesterol synthesis, as well as inflammation. The BECCs obtained from this study may shed light on the selection of appropriate marker compounds for quality control of citrus products.

Conflicts of interest

The authors declare no conflict of interest.

Acknowledgment

We greatly appreciate financial support from the National Key Research and Development Program of China (2017YFC1701105 and 2017YFC1701103), National Natural Science Foundation of China (81922072 and 81973443), "Double First-Class" University project (CPU2018PZQ16 and CPU2018GF04), and a Project Funded by the Priority Academic Program Development of Jiangsu Higher Education Institutions.

Appendix A. Supplementary data

Supplementary data to this article can be found online at <https://doi.org/10.1016/j.clnesp.2021.03.023>.

References

- [1] Fu MQ, Xu YJ, Chen YL, Wu JJ, Yu YS, Zou B, et al. Evaluation of bioactive flavonoids and antioxidant activity in Pericarpium Citri Reticulatae (Citrus reticulata 'Chachi') during storage. *Food Chem* 2017;230:649–56.

- [2] Sun YS, Wang JH, Gu SB, Liu ZB, Zhang YJ, Zhang XX. Simultaneous determination of flavonoids in different parts of *Citrus reticulata* 'chachi' fruit by high performance liquid chromatography-photodiode array detection. *Molecules* 2010;15:5378–88.
- [3] Ho SC, Kuo CT. Hesperidin, nobiletin, and tangeretin are collectively responsible for the anti-neuroinflammatory capacity of tangerine peel (*Citrireticulatae pericarpium*). *Food Chem Toxicol* 2014;71:176–82.
- [4] Tripoli E, Guardia ML, Giammanco S, Majo DD, Giammanco M. Citrus flavonoids: molecular structure, biological activity and nutritional properties. *Food Chem* 2007;104:466–79.
- [5] Zeng SL, Li SZ, Lai CJS, Wei MY, Chen BZ, Li P, et al. Evaluation of anti-lipase activity and bioactive flavonoids in the citri reticulatae pericarpium from different harvest time. *Phytomedicine* 2018;43:103–9.
- [6] Zhang M, Zhu JY, Zhang X, Zhao DG, Ma YY, Li DL, et al. Aged citrus peel (chenpi) extract causes dynamic alteration of colonic microbiota in high-fat diet induced obese mice. *Food Funct* 2020;11:2667–78.
- [7] Guo J, Tao H, Cao Y, Ho CT, Jin S, Huang Q. Prevention of obesity and type 2 diabetes with aged citrus peel (chenpi) extract. *J Agric Food Chem* 2016;64:2053–61.
- [8] Long F, Yang H, Xu Y, Hao H, Li P. A strategy for the identification of combinatorial bioactive compounds contributing to the holistic effect of herbal medicines. *Sci Rep* 2015;5:12361.
- [9] Xu Z. Modernization: one step at a time. *Nature* 2011;480:S90–2.
- [10] Liang XM, Jin Y, Wang YP, Jin GW, Fu Q, Xiao YS. Qualitative and quantitative analysis in quality control of traditional Chinese medicines. *J Chromatogr A* 2009;1216:2033–44.
- [11] Gao Z, Wang ZY, Guo Y, Chu C, Zheng GD, Liu EH, et al. Enrichment of polymethoxyflavones from citrus reticulata 'chachi' peels and their hypolipidemic effect. *J Chromatogr B* 2019;1124:226–32.
- [12] Liu P, Yang H, Long F, Hao HP, Xu XJ, Liu Y, et al. Bioactive equivalence of combinatorial components identified in screening of an herbal medicine. *Pharm Res (NY)* 2014;31:1788–800.
- [13] Guo L, Duan L, Dou LL, Liu LL, Yang H, Liu EH, et al. Quality standardization of herbal medicines using effective compounds combination as labeled constituents. *J Pharmaceut Biomed* 2016;129:320–31.
- [14] Klymenko T, Brandenburg M, Morrow C, Dive C, Makin G. The novel Bcl-2 inhibitor ABT-737 is more effective in hypoxia and is able to reverse hypoxia-induced drug resistance in neuroblastoma cells. *Mol Cancer Therapeut* 2011;10:2373–83.
- [15] Liu EH, Zhao P, Duan L, Zheng GD, Guo L, Yang H, et al. Simultaneous determination of six bioactive flavonoids in citri reticulatae pericarpium by rapid resolution liquid chromatography coupled with triple quadrupole electrospray tandem mass spectrometry. *Food Chem* 2013;141:3977–83.
- [16] Duan L, Dou LL, Yu KY, Guo L, Chen BZ, Li P, et al. Polymethoxyflavones in peel of citrus reticulata 'chachi' and their biological activities. *Food Chem* 2017;234:254–61.
- [17] He BK, Nohara K, Park N, Park YS, Guillory B, Zhao ZY, et al. The small molecule nobiletin targets the molecular oscillator to enhance circadian rhythms and protect against metabolic syndrome. *Cell Metabol* 2016;23:610–21.
- [18] Soyal SM, Nofziger C, Dossena S, Paulmichl M, Patsch W. Targeting SREBPs for treatment of the metabolic syndrome. *Trends Pharmacol Sci* 2015;36:406–16.
- [19] Repa JJ, Berge KE, Pomajzl C, Richardson JA, Hobbs H, Mangelsdorf D. Regulation of ATP-binding cassette sterol transporters ABCG5 and ABCG8 by the liver X receptors alpha and beta. *J Biol Chem* 2002;277:18793–800.
- [20] Venkateswaran A, Laffitte BA, Joseph SB, Mak PA, Wilpitz DC, Edwards PA, et al. Control of cellular cholesterol efflux by the nuclear oxysterol receptor LXR alpha. *P Natl Acad Sci USA* 2000;97:12097–102.
- [21] Chi L, Lai YJ, Tu PC, Liu CW, Xue JC, Ru HY, et al. Lipid and cholesterol homeostasis after arsenic exposure and antibiotic treatment in mice: potential role of the microbiota. *Environ Health Perspect* 2019;127:97002.
- [22] Dai JY, Liang K, Zhao S, Jia WT, Liu Y, Wu HK, et al. Chemoproteomics reveals baicalin activates hepatic cpt1 to ameliorate diet-induced obesity and hepatic steatosis. *P Natl Acad Sci USA* 2018;115:E5896–905.
- [23] Xiao PT, Liu SY, Kuang YJ, Jiang ZM, Lin Y, Xie ZS, et al. Network pharmacology analysis and experimental validation to explore the mechanism of sea buckthorn flavonoids on hyperlipidemia. *J Ethnopharmacol* 2021;264:113380.
- [24] Feng KL, Zhu XA, Chen T, Peng B, Lu MW, Zheng H, et al. Prevention of obesity and hyperlipidemia by heptamethoxyflavone in high-fat diet-induced rats. *J Agric Food Chem* 2019;67:2476–89.
- [25] Zeng SL, Li SZ, Xiao PT, Cai YY, Chu C, Chen BZ, et al. Citrus polymethoxyflavones attenuate metabolic syndrome by regulating gut microbiome and amino acid metabolism. *Sci Adv* 2020;6:eaa6208.